Pumpkin seeds as an eco-friendly corrosion inhibitor for 7075-T6 alloy in 3.5% NaCl solution: electrochemical, surface and computational studies.

RADI, M., MELIAN, R., GALAI, M., DKHIRCHE, N., MAKHA, M., VERMA, C., FERNANDEZ, C. and EBN TOUHAMI, M.

2021

Pumpkin seeds as an Eco-Friendly Corrosion Inhibitor for 7075-T6 alloy in 3.5% NaCl Solution: Electrochemical, Surface and Computational studies

M.Radi[a,], R.Melian[a] ,M.Galai[a,*],N.Dkhirche[a], M. Makha [b], ChandrabhanVerma[c],**

C.Fernandez[d], M.EbnTouhami[a]

[a]*Advanced Materials and Process Engineering Laboratory, Faculty of Science, Ibn Tofail University, BP.133-140 0 0 Kenitra, Morocco*

[b]*Materials Science, Energy and Nano-engineering Department, Mohammed VI Polytechnic University (UM6P), Lot 660, Hay Moulay Rachid, Bengurir, 43150, Morocco*

c *Center of Research Excellence in Corrosion, Research Institute, King Fahd University of Petroleum*

and Minerals, Dhahran, 31261, Saudi Arabia

[d]*School of Pharmacy and Life Sciences Robert Gordon University, Aberdeen (UK) – AB10 7GJ.*

✉**Corresponding authors**

Dr. M.Galai*E-mail : galaimouhsine@gmail.com   **Phone:** 00212677235695
Dr. M.Radi **E-mail:** radi.morad@gmail.com

ABSTRACT:

For the aeronautics industry, constraints of mechanical strength are paramount. Aluminum and its alloys are widely used for various household and industrial applications. Among the various established and identified aluminum alloys, 7075 alloy, which is an aluminum-zinc, acquires the best mechanical strength. However, this is sensitive to certain localized corrosion phenomena such as pitting corrosion. Pumpkin seeds (PS) were evaluated as a corrosion inhibitor for aluminum alloy 7075-T6 in 3.5% NaCl solution using electrochemical, surface and theoretical studies. PS showed highest inhibition efficiency of 95% at its 1g/L concentration (298K). Furthermore, the Pumpkin seeds (PS) acted as a cathodic inhibitor. Adsorption of Pumpkin seeds (PS) on Aluminum alloy surface corresponds to the Langmuir adsorption isotherm. Surface studies carried out using scanning electron microscope (SEM), atomic force microscope (AFM) and X-ray Diffraction (XRD) provide good supports to the polarization and EIS studies. Surface studies also validate that PS becomes effective by adsorbing on the metallic surface. Using DFT investigation, it was derived that effectiveness of the major phytochemical followed the sequence: 9,12-Octadecadienoic acid (Z, Z)-> linoleic acid > palmitic acid.

Keywords: AA7075-T6, Pumpkin Seeds, corrosion, inhibition,computational simulations, cathodic-type and Langmuir adsorption isotherm.

1. Introduction

Alloying of aluminum improves its physiochemical properties. One of the major improvements of alloying of aluminum is to increase its mechanical strength. Iron, silicon, copper, magnesium, manganese, and zinc are the major alloying components that constitute around 15% of total aluminum alloy weight. This alloy is identified by a four-digit number in which the first digit gives identity to a series featured by its major alloying components. The use of aluminum and its alloys is widespread in the industry, especially in the aeronautical sector. The surface treatment is often necessary to form a protective layer on the material surface, an anodic oxidation operation so called anodization is employed. This is usually made using a stripping/degreasing treatment and followed by a sealing step to ameliorate the oxide layer's corrosion resistance and form a porous layer consisting of $Al(OH)_3$ amorphous structure and crystallized Al_2O_3. 7000 alloys are aluminum-zinc alloys with or without copper. We will be interested in 7000 alloys containing copper, the family to which the studied 7075 alloys belong. These alloys own the highest mechanical properties of all aluminum alloys, but they have poor corrosion resistance [1].Several authors [2-4] have demonstrated the presence of Al_7Cu_2Fe and (Al, Cu) 6 (Fe, Cu) intermetallic compounds in 7000 alloys containing copper. These compounds are distributed in grains. They have irregular shapes and sizes ranging from 1 to 20 microns [5]. Round particles of Mg_2Si of sizes between 1 and 10μm have been identified [2,5].

The inhibition of corrosion of aluminum alloys 7000 has been the subject of earlier works. Among the most commonly used inhibitors we cite chromates, silicates, and molybdates [6,7]. Experimental techniques such as electrochemical and surface analysis methods have contributed to the best understanding of the mechanism inhibition of these ions, but most of them are highly toxic for humans and the environment. These inhibitors may damage the system organ and may disrupt the corps' enzymatic system [8]. Consequently, plant extracts are increasingly viewed as green corrosion inhibitors' origin to replace the toxic chemicals currently employed concerning environmental concerns[9].Pumpkins are members of the Cucurbitaceae family. Pumpkin seeds and seed oil give many benefits to health due to their different composition [10]. They are considered a valuable natural source of proteins, phytosterols, polyunsaturated fatty acids [11], antioxidants, vitamins, and trace elements [12]. Several studies have carried out on the protection of corrosion of metals and alloys by plant extracts. The present study seeks to investigate Pumpkin seeds' effectiveness against the corrosion of AA7075-T6 in a 3.5% NaCl solution.

2. Experimental

2.1. Preparation of Inhibitor

Pumpkin seeds were washed to remove impurities, and they were dried. Then, they were transformed into powder through grinding. The powder was sifted. The powder obtained was analyzed by Fourier Transform Infrared Spectroscopy (FTIR) and Gas Chromatography-Mass Spectrometry (type QP2010 Shimadzou) and by Trace gas chromatography / Polaris Q (Gas Chromatography-Mass Spectrometry, Thermo-Electron).

The samples' FTIR spectra were recorded with a VERTEX 70 device, in the wavelength range of 400 to 4000cm^{-1} and using the attenuated total reflection mode (ATR). The powder was pelletized at about 1% by weight in potassium bromide (KBr) previously stored in an oven at 100°C and under a pressure of about 1000psi (pound-force per square inch).The gas chromatographic column used helium as a mobile phase. It had 95% dimethyl polysiloxane and 5% phenyl, with a length of 30m, a layer thickness of 0.25μm, and an interior diameter of 0.24μm.

2.2. Materials and solutions

Electrochemical measurements were carried out in a three-electrode type cell (Ag/AgCl, 3M concentration in Cl$^-$) used as the reference electrode, although platinum (Pt) as the counter electrode. The working electrode is AA7075-T6 with an exposure area of 1cm^2, prepared by grinding with abrasive SiC paper (gradation 180,220,360,600,1200,1500,2000), rinsed with distilled water and degreased. Before each measurement, the sample was immersed in a corrosion cell to stabilize for two hours.

The pumpkin seeds were easily dissolved at ambient temperature in acetone. Amounts 250, 500, 1000, and 1500ppm of this inhibitor were prepared using 3.5% of NaCl solution (chlorinated medium)

The AA7075-T6 was used with the composition (weight %) as presented in Table1:

Table 1. Chemical composition of AA7075-T6 used in weight %

Zn	Mg	Cu	Cr	Mn	Ti	Si	Fe	Al
5.81	2.62	1.59	0.19	0.01	0.02	0.08	0.23	Balance

2.3. Polarization measurements:

The Aluminum alloy electrode was immersed in the solution for two hours until the evolution of the open circuit potential (Eocp) as a function of time was constant. The cathodic polarization curve was registered by polarization from E_{ocp} to negative with a sweep rate of 1mV/s. The same electrode remained in solution after this scan until the steady state of the corrosion potential reached Eocp ± 0.02V. Then, the anodic polarization curve was recorded

from Eocp towards the positive direction with the same sweep rate. These measurements were done using a Potentiostat PGZ 100 monitored by a personal computer. For each concentration, three independent experiments were performed. The Tafel extrapolation method of the linear part of the cathodic domain was utilized to extract the corrosion parameters. The corrosion inhibition efficiency is measured from the corrosion current density values employing the relationship (1):

$$\eta = \frac{i_{corr}^0 - i_{corr}}{i_{corr}^0} \times 100 \tag{1}$$

i_{cor}^0 and i_{cor} are the corrosion current density values without and with the inhibitor pumpkin seeds.

2.4. EIS measurements:

The electrochemical impedance spectroscopy SIE measurements obtained by the analyzer (Voltalab PGZ 100), the frequency from 100kHz to 0,01Hz with 10 points per decade, amplitude AC signal was 30mV. All measurements were performed at the open circuit potential. The obtained impedance data was investigated by a similar electrical circuit using Bouckamp's program **[13].** The inhibition efficiency was calculated from Rp as indicated by equation 2:

$$\eta = \frac{R_p - R_p^0}{R_p} \times 100 \tag{2}$$

R_p^0 and R_p are the polarization resistance values without and with inhibitor pumpkin seeds, respectively.

2.5. Surface study

The AA7075-T6 is immersed in NaCl 3.5% in the inhibitor's absence and presence to analyze the corrosion and inhibition effects on the surface morphologies. The AA7075-T6 were dried at ambient temperature. Micrographs of corroded Aluminum alloy surfaces and those after inhibitor addition were observed using an SEM model (SEM; JOEL JSM-5500).

AFM analysis was performed on the aluminum alloy 7075-T6 surface to verify the roughness of the surface. Images were processed using Gwyddion software. The AA7075-T6 samples surface was immersed for 20h in the blank and inhibited solution. The examination of the AA7075-T6 sample's surface was carried out using the XRD X' PERT PRO MPD model.

2.6. Computational study

2.6.1 DFT calculations

DFT based quantum chemical calculations (QCCs) were carried out to demonstrate the corrosion inhibition potential of some major phytochemicals namely, (Z,Z)-9,12-Octad-ecadienoic acid, palmitic acid and linoleic acid for AA7075-T6 in 3.5% sodium chloride

solution. DFT study was conducted in solvated phase using Gaussian 09 software package involving B3LYP functional and 6-31G (d,p) basis set. DFT analysis of three major phytochemicals was conducted. Using DFT investigations, interactions efficiency of 9,12-Octadecadienoic acid, palmitic acid and linoleic acid with aluminum surface was investigated. Various chemical reactivity parameters including, energies of FMOs (frontier molecular orbitals) i.e. E_{HOMO}; the energy of highest occupied molecular orbital, E_{LUMO}; the energy of lowest unoccupied molecular orbital, ΔE; energy band gap (E_{LUMO}-E_{HOMO}), IP; ionization potential, EA; electron affinity, η; hardness, σ softness, electronegativity and μ; dipole moment were derived using following relationships [14-16]:

$$IP = -E_{HOMO} \tag{3}$$

$$EA = -E_{LUMO} \tag{4}$$

$$\chi = -1/2\left(E_{HOMO} + E_{LUMO}\right) \tag{5}$$

$$\eta = -\left(E_{HOMO} - E_{LUMO}\right) \tag{6}$$

$$\sigma = \frac{1}{2\eta} \tag{7}$$

3. Results and discussion

3.1. Chemical composition and characterization of Pumpkin Seeds

Figure1 show the vibration bands of pumpkin seeds. Fourier Transform Infrared Spectroscopy (FTIR) spectral data for PS are given in (Table 2).
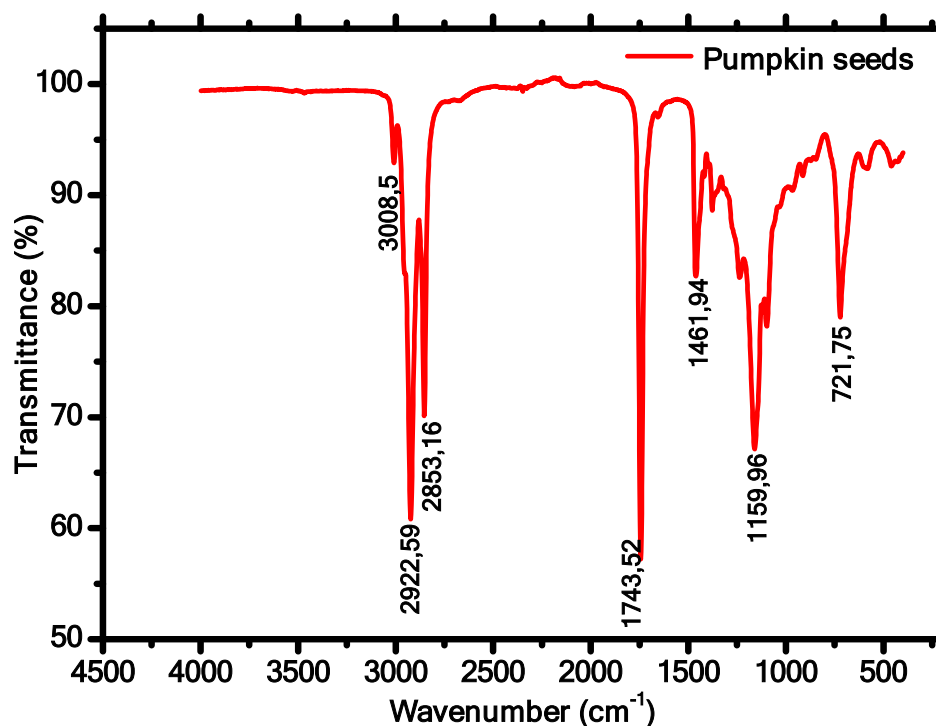

Fig.1. Spectrum IR of pumpkin seeds

Table2. Attribution of the main IR characteristic bands of pumpkin seeds

Wave number cm^{-1}	Bond	Intensity
3008.5	C$_{\text{éne}}$-H	92.9
2922.59	C$_{\text{ane}}$-H	60.8
2853.16	C$_{\text{ane}}$-H	70.1
1743.52	C=O	57.2
1461.94	C$_{\text{tet}}$-H	82.7
1159.96	C-C	67.1
721.75	C-H	79

The analysis of the IR spectrum of pumpkin seeds shows the presence of an asymmetrical band located at 2853cm^{-1} and another asymmetric band located around 2922cm^{-1}, both corresponding to the elongation vibration of the bond (C-H). The vibration of the bonds' deformation (C-H) has led to a band in the plan located at 1461cm^{-1} and another out of the plan located at 1461cm^{-1}. Also, a vibration band was located at 1743 attributed to a C = O bond. Figure 2 shows the spectrum of gas chromatography and gas chromatography-mass spectroscopy of the PS dissolved in dichloromethane (CH$_2$Cl$_2$).
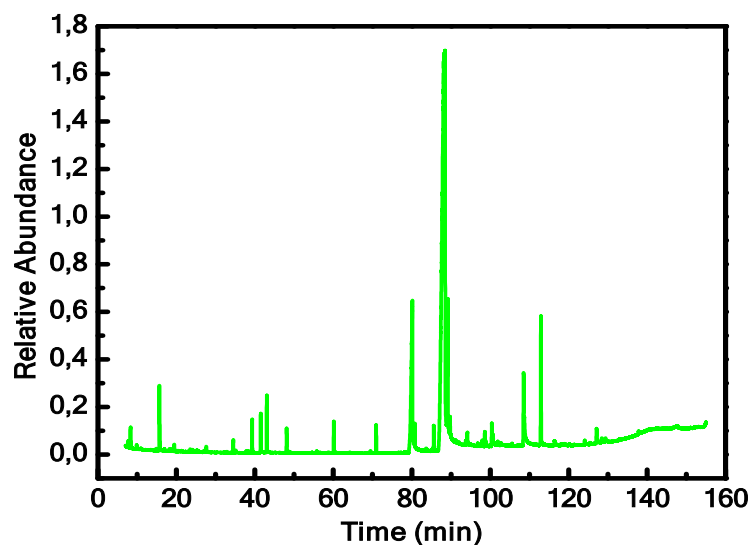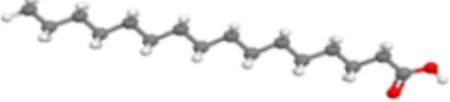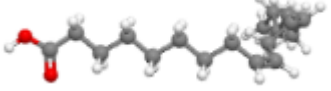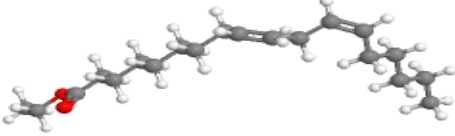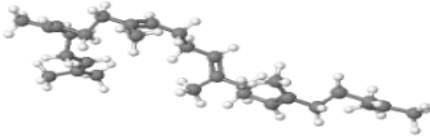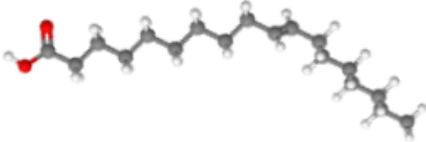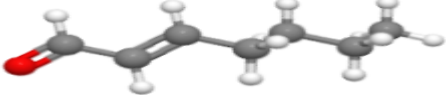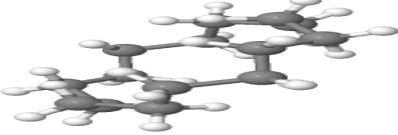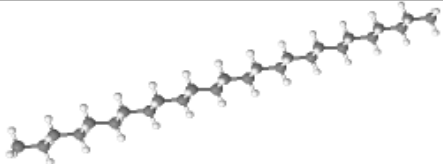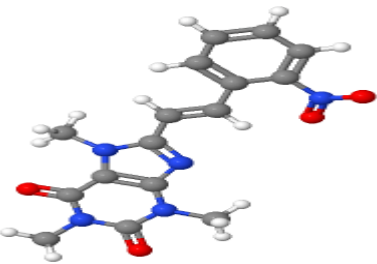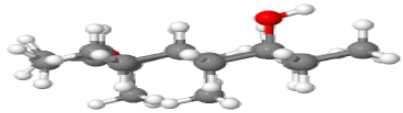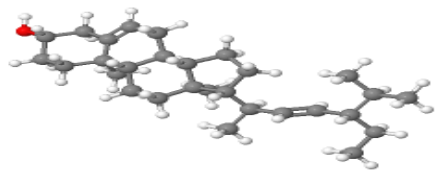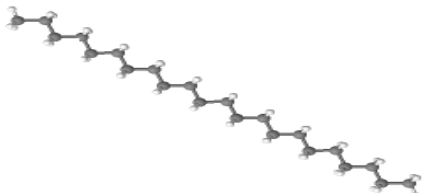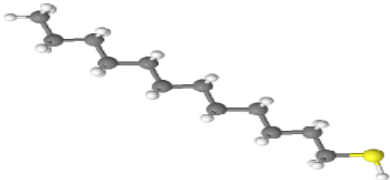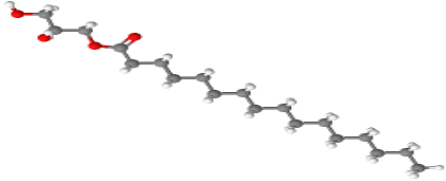

Fig.2. The spectrum of gas chromatography and gas chromatography-mass spectrometry of PS

Table 3. Chemical compounds identified in PS by GC–MS analysis

Compounds name	percentage %	Molecular weight (g/mol)	The chemical structures
9,12-Octadecadienoic acid (Z,Z)-	57,36	280 ($C_{18}H_{32}O_2$)	
Palmitic acid	13,03	*256* ($C_{16}H_{32}O_2$)	
Linoleic acid	3,67	*280* ($C_{18}H_{32}O_2$)	
Ethyl (9Z,12Z)-9,12-octadecadienoate	3,22	*308* ($C_{20}H_{36}O_2$)	
Squalene	2,48	410 ($C_{30}H_{50}$)	
Octadecanoic acid	2,32	284 ($C_{18}H_{36}O_2$)	
Stearic acid	1,8	284 ($C_{18}H_{36}O_2$)	
2-Heptenal, (E)-	1,5	112 ($C_7H_{12}O$)	
(2E,4E)-deca-2,4-dienal	1,45	152 ($C_{10}H_{16}O$)	
(2E,6Z)-nona-2,6-dienal	1,2	138 ($C_9H_{14}O$)	
Cyclotetradecane	1,14	196 ($C_{14}H_{28}$)	

Hexacosane	1,02	366 ($C_{26}H_{54}$)	
Purin-2,6-dione,1,3,9-trimethyl-8-[2-nitrophenethenyl]-	0,9	341 ($C_{16}H_{15}N_5O_4$)	
Androstan-17-one, 3-ethyl-3-hydroxy-, (5.alpha.)-	0,86	318 ($C_{21}H_{34}O_2$)	
Stigmasterol	0,82	412 ($C_{29}H_{48}O$)	
Undecane	0,77	156 ($C_{11}H_{24}$)	
Docosane	0,72	310 ($C_{22}H_{46}$)	
1-Docosanethiol	0,7	342 ($C_{22}H_{46}S$)	
(2S)-2,3-dihydroxypropyl hexadecanoate	0,61	330 ($C_{19}H_{38}O_4$)	

Chromatographic analysis of PS by GC/MS showed the presence of **52** compounds, including 9,12-Octadecadienoic acid (Z, Z)- **(57.36%)**, Palmitic acid **(13.03%)**, Linoleic acid **(3.67%),** and Ethyl (9Z, 12Z) -9,12-octadecadienoate **(3.22%)** being the main constituents, these molecules are shown in table 3.

9,12-Octadecadienoic acid (Z, Z)-is a good antioxidant compound **[17].**The major chemical compounds identified in PS have been present in diverse plant species, as in the case of 9,12-

Octadecadienoic acid (Z,Z)-, the most abundant in the extract of garlic (40,52 % in the total), and identified in Scenedemusalge.

The other major chemical compounds of PS: octadecanoic acid, stearic acid, and Linoleic acid. These fatty acids have been studied as corrosion inhibitors. Also, various components minor such as 1-Docosanethiol, Purin-2,6-dione,1,3,9-trimethyl-8-[2-nitrophenethenyl]-**[18].**

These compounds comprise oxygen, sulfur, nitrogen as heteroatom and aldehyde functional groups, and this heteroatom possesses free electron pairs. Furthermore, pumpkin seeds are devoid of toxicity **[19-21].**

3.2. Electrochemical measurements

3.2.1. Potentiodynamic polarization measurements

Firstly, we have studied the inhibition of AA7075-T6 under different concentrations of the PS. Figure 3 presents the current density as a function of potential with different concentrations (0, 0.25, 0.5, 1 and 1.5g/L).
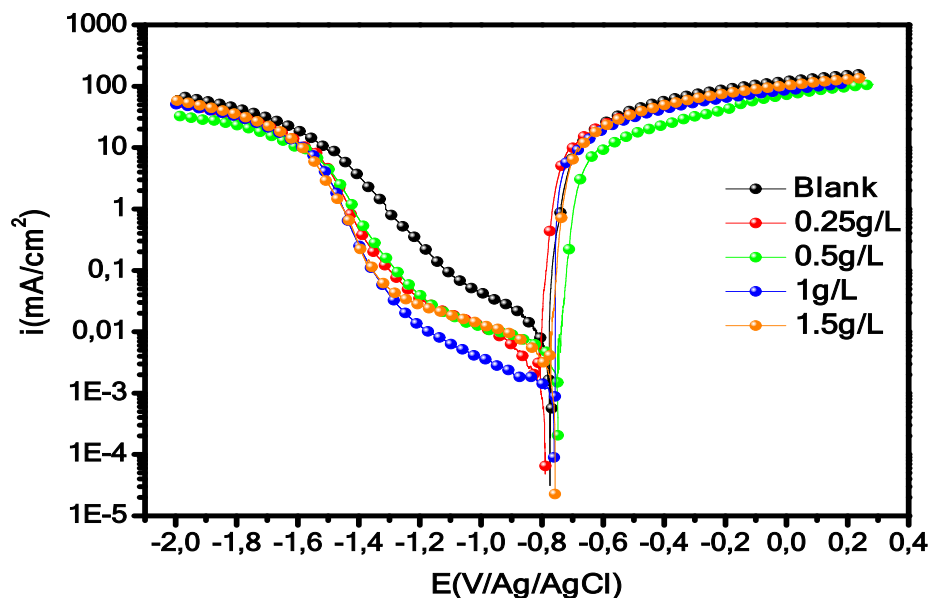
Fig.3. Polarization curves for AA7075-T6 in NaCl 3.5 % after 2 hours of immersion at 298K without and with different concentrations of PS, $|dE/dt| = 1$ mV.s^{-1}.

Focusing on the concentration effect, we have seen that, in a wide domain, the current density decreases as the concentration increases, reaches its maximum of 1g/L. The domain from -1.2 to -0.9V, which we can consider as linear indicates that the change happens in kinetic control during the cathodic reaction. This comportment may be attributed to the formation of a film that acts as a diffusion barrier and limits oxygen reduction. Indeed, the reduction plateau observed without inhibitor is obtained only at high cathodic overvoltage. The diminution in cathodic current density indicates that the inhibitor is cathodic. Table 4 illustrates the electrochemical parameters (the corrosion potential (E_{corr}), corrosion current density (i_{corr}), slope cathodic (bc), and the inhibition efficiency ($\eta\%$) for AA7075-T6 in NaCl 3.5% containing various concentrations of PS at 298K.The Tafel extrapolation method of the linear

part was used (cathodic domain) in Pumpkin Seeds' absence and presence. The values of inhibition efficiency were calculated from the relation as shown in Eq (1).

Table 4. Electrochemical parameters for AA7075-T6 in NaCl 3.5% in various concentrations of PS at 298 K.

	E_{corr}(mV/Ag/AgCl)	i_{corr}(μA/cm^2)	$-\beta c$(mV)	EI%
Blank	-773.7	10.81	359.3	
0.25	-742.8	5.26	680.3	51.34
0.5	-784.7	2.2	266.9	79.64
1	-745.12	0.79	369.6	92.7
1.5	-751.05	3.74	401.2	65

We can observe that the increase of PS concentration leads to a decrease in the corrosion current density. The inhibition efficiency reaches 92.7% at 1g/L. In this case, the adsorption rate of PS remains higher than its desorption rate. The posterior diminution in the inhibition efficiency value for the concentration 1.5g/L is due to the desorption of the inhibitor molecules from the alloy's surface. It can also be due to the reinforcement in corrosion on a relatively small area of the alloy Aluminum surface, which is not protected by the inhibitor. Comparing to the efficiency of other inhibitors such as plant-derived cationic dye (78%) **[22],** Date Palm (Phoenix dactyllifera L.), and Fruit Juice (63%) **[23],** the inhibition efficiency obtained in this study has improved the protection against corrosion.

3.2.2. Electrochemical Impedance Spectroscopy:

The corrosion of AA7075-T6 in 3.5% NaCl solution in the absence and presence of PS was also studied by electrochemical impedance spectroscopy (EIS) at 298±2K. Nyquist plots of Aluminum in uninhibited solution and containing various concentrations of PS are given in Fig4:
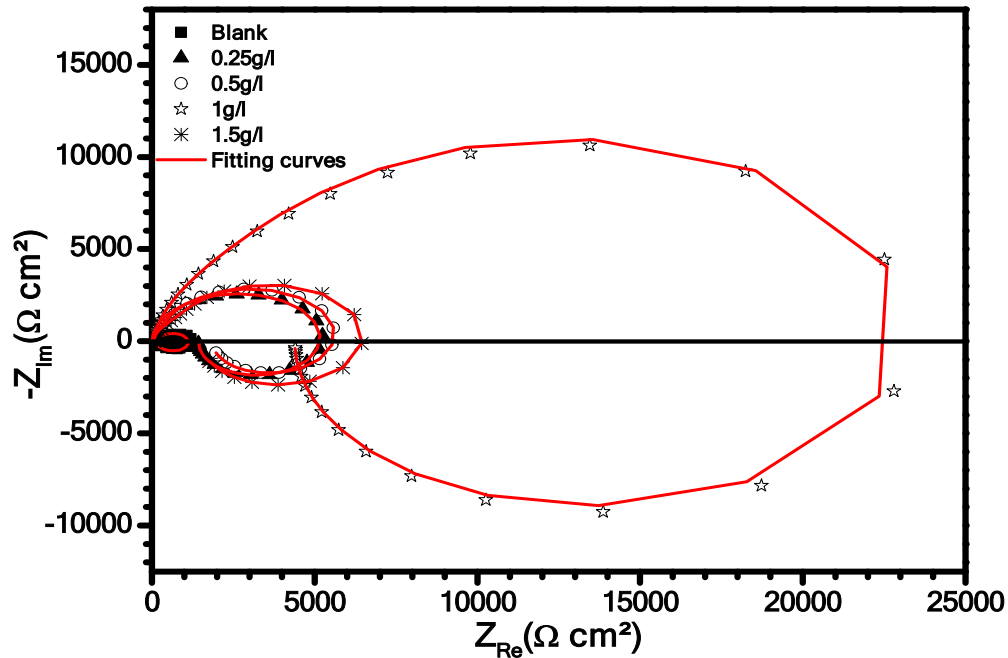
Fig.4. Nyquist plots of AA7075-T6 in 3.5% NaCl solution with and without various concentrations of PS.

The impedance response of AA7075-T6 in NaCl 3.5% solution was changed after the addition of inhibitor, and the size of the impedance spectra of the inhibited solution increased with the inhibitor concentration.

The impedance diagrams in the existence of PS consist of three loops. At high and medium frequencies, we noticed two loops: relatively bad separated and an inductive loop at the lowest frequencies. To confirm this result, we have traced the bode plot for these spectra (Fig.5). From this figure , the Bode plots show two-phase maxima (i.e.Two times constant) at intermediate and high frequencies.

For more clarity, the first loop capacitive might be assigned to the formation of the protective film. The second can be attributed to the double layer's relaxation that is parallel with the charge transfer resistance at the medium frequencies. The inductive loop in lower frequency may be attributed to the adsorption's relaxation process on the Aluminum surface [24, 25].Nevertheless, based on the work of Chen and his collaborators, the appearance of an inductive phenomenon could also be possible in the case of the association of electrochemical and chemical phenomenon: this can be the case of a growing phenomenon of an oxide associated with its dissolution in the electrolyte [26].The simulation data of the AA7075-T6 immersed in (0.25, 0.5, 1, and 1.5 g/L) of PS in 3.5% NaCl solution after 2hours are presented as Bode in Fig.5:
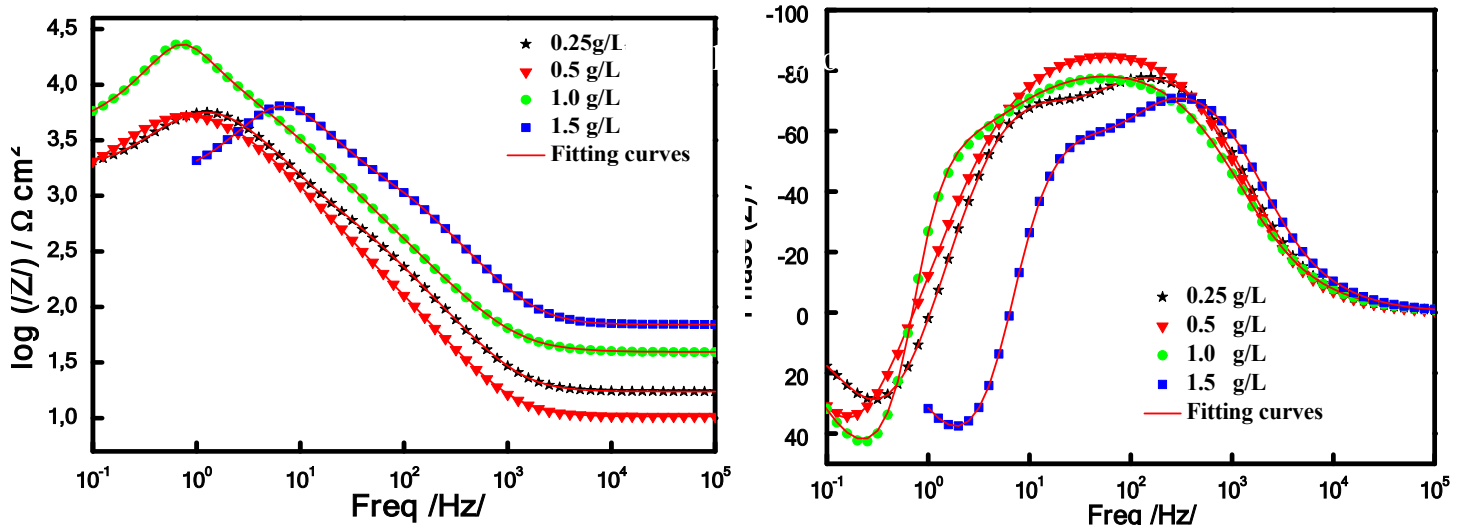
Fig.5. Bode plots of AA7075 in NaCl 3.5% with various concentration of PS.

Using the Bouckamp's program to simulate the EIS diagrams, one equivalent circuit was utilized Fig.6, the capacitor replaced by a constant phase element, which designates the existence of dissimilar frequency response, the equation 8 represented the CPE impedance **[27].**

$$Z_{CPE}(\omega) = Q^{-1}(j\omega)^{-n} \tag{8}$$

$Q(\Omega.cm^{-2}.sn)$: a constant.

$\omega(rad.s^{-1})$: the angular frequency.

$n(-1 < n < 1)$: the CPE exponent.

The elements form the equivalent circuit are: (**R**s: the solution resistance, **R**f: the film resistance, **R**ct: the charge transfer resistance, **CPE** the constant phase elements, **n** represent a depressing feature in the Nyquist diagrams, **L** the inductance, **R**L the inductive resistance.

The polarization resistance **(Rp)** was calculated using the following equation 9:

$$R_p = R_f + R_{ct} + R_s \tag{9}$$
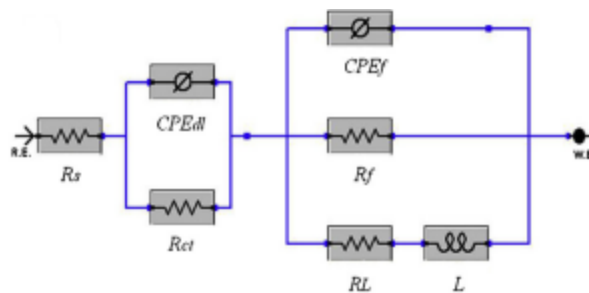
Fig.6.model of the equivalent circuit for fitting the data experimental.

	R_S	nF	C_f	R_f	Q_f	N_{ct}	C_{ct}	R_{ct}	Q_{ct}	R_L	L	R_P	EI%
Blank	12.53	1	107.3	107.3	170.3	0.90	-	1111		16	211	1218	
0.25	17.34	0.99	19.39	231.9	17.83	0.98	14.28	5691	10.96	2227	2038	5923	79
0.5	10.33	0.95	134.8	2255	71.73	0.99	17.95	3801	16.06	687.7	1477	6056	79
1	39.21	0.89	50.48	3487	13.37	1	9	20353	9	905.2	5641	23840	95
1.5	69.4	1	2.44	693.4	2.44	0.99	2.91	6060	2.64	833.8	233.8	6753	82

R_s, R_{ct} ,R_f, R_L and R_p ,are expressed in $\Omega.cm^2$

C_f ,C_{ct} are given in $\mu F\ cm^{-2}$

Q_f and Q_{ct} are expressed $\mu F\ cm^{-2}S$

L is expressed in H.

From the table5, the values of C_{ct} and C_f decrease by increasing inhibitor concentrations of pumpkin seeds, while $R_{ct}$ and R_f's values increased. The significant decrease in the capacitance values can be attributed to an increase in the double electric layer thickness due to the inhibitor PS's adsorption on aluminum alloy surface or a decrease in the dielectric constant [28].

The electrolytic resistance Rs change with the increase of the inhibitor concentration PS and decrease until the optimum value. The authors propose that Rs' change possibly to the galvanic coupling between the local cells once the molecules of inhibitor PS are adsorbed more and more on the active sites of AA7075-T6 surface and develop a denser film progressively and as a result to great inhibiting efficiency [29].

The inhibition efficiency increases with the presence of inhibitor PS. The polarization resistance R_p increases with the addition of inhibitor show the adsorption of inhibitor molecules at the Alloy/electrolyte interface [30].

3.2.3. Adsorption isotherm:

The Langmuir isotherm presents the best appropriate with the experimental data obtained. The Langmuir isotherm equation is given by the equations [31].

$$\frac{C}{\theta} = \frac{1}{K} + C \tag{10}$$

$$K = \frac{1}{55,5} \exp\left[\frac{-\Delta G°ads}{RT}\right] \tag{11}$$

θ is the degree of surface coverage, K_{ads} is the equilibrium constant of the process of adsorption, and C the molar inhibitor concentration. The variation of the ratio Cinh/ θ as a function of inhibitor concentration is linear (Fig.7).
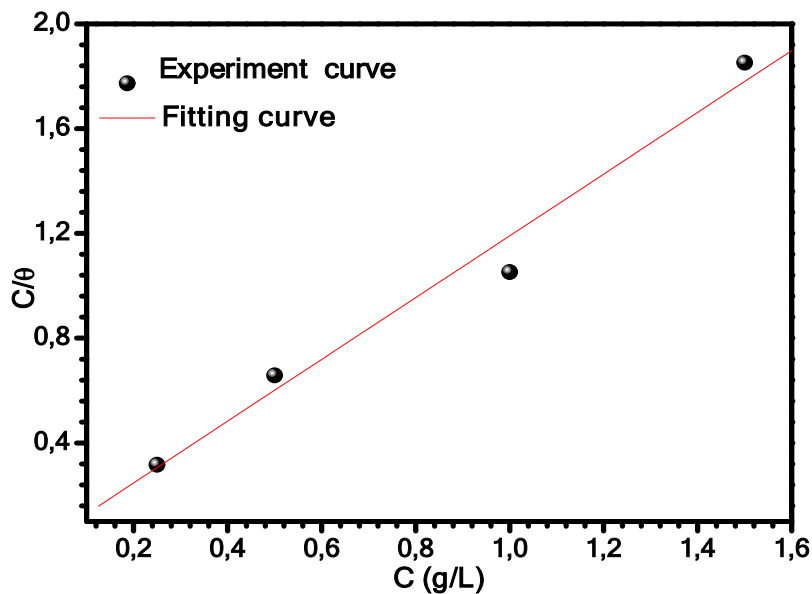
Fig.7. isotherm adsorption of Langmuir (C/θ vs. C) of PSin 3.5% NaCl at 298K.

Table 6. Parameters Thermodynamic for the adsorption of PS in NaCl 3.5% on the AA7075-T6 at 298K.

	KadsKj/mol	ΔG ads Kj/mol	R²
Langmuir	85.10	-20.9	0.99

The coefficient of correlation R^2 presents the degree of fit between the experimental data and the equation isotherm, the value obtained 0.99 indicates a very good appropriate between the data experimental and the Langmuir isotherm.

In general, the values of ΔG_{ads} (20Kj/mol or inferior) are consistent with the electrostatic interaction between the molecules charged and the electrode (physisorption) and the values of ΔG_{ads} (40Kj/mol or superior) are consistent with transfer from organic molecules to the electrode surface (chemisorptions) **[32,33].**

The ΔG_{ads} values slightly negative of 20 Kj/mol show that the Pumpkin seeds' adsorption action on Aluminum alloy in NaCl 3.5% solution was physisorption (Table 6).

3.2.4. Effect of temperature:

3.2.4.1. Polarization curves:

Given the importance of the temperature factor, an electrochemical study on the comportment of alloy 7075 in NaCl 3.5% without and with inhibitor for temperatures between 298 and 328K was carried out. The obtained polarization curves are presented in Fig 8:
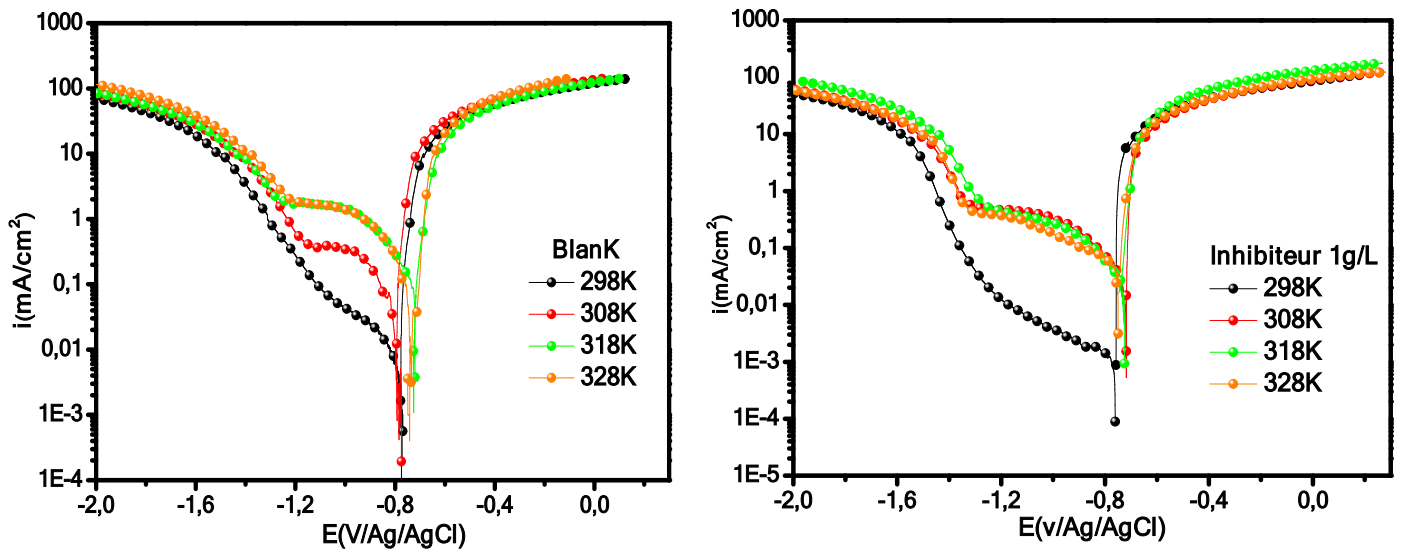
Fig.8. curves Potentiodynamic polarization of AA7075-T6 in NaCl 3.5 % without and with the PS 1g/L at various temperatures.

The impact of temperature on inhibition reaction is complex, for many reactions may occur on the electrode surface for example rupture and desorption of molecules inhibitor. The curves in the cathodic and anodic part are made according to the same mechanism in the whole temperature range

Table 7. parameters Electrochemical of AA7075-T6 in NaCl 3.5 % with and without PS at various temperatures.

Medium		Temperature	$-E_{corr}$ (mV/ECS)	i_{corr} ($\mu A/cm^2$)	$-\beta c$ (mv/dec)	βa (mv/dec)	E%
3.5% NaCl	Blank	298 k	-773.7	10.8	359.3	216.1	-
		308 k	-773.6	76.7	302.1	157	-
		318 k	-716.3	143.6	235	186.3	-
		328 k	-731.2	171.1	247.3	182	-
	Pumpkin Seeds 1g/L	298 k	-744.6	0.5	200	258.7	95
		308 k	-717.9	10.6	50.8	61.1	86
		318 k	-726.7	25.4	78.1	41.4	82
		328 k	-746.9	34.1	140.4	42	80

The corresponding data are collected in table7, the evolution in corrosion currents in the corrosive solution alone (3.5% NaCl) presents a fast and regular development, confirming a growing metallic dissolution with the increase of temperature. Moreover, no clear trends are observed in E_{corr} values. The increase in corrosion current with temperature in the presence of inhibitor is widely lower than in the without inhibitor.

3.2.4.2. Thermodynamic part:

The dependence of the logarithm of corrosion rates (LnCR) on the reciprocal of the absolute temperature (1/T) for blank and pumpkin seeds was examined. The plots obtained are Linear (Fig. 9), which shows the Arrhenius equation **[34-36].**

$$LnCR = -\frac{Ea}{RT} + LnA \tag{12}$$

A: the Arrhenius pre-exponential constant.

R: the universal gas constant.

T: the absolute temperature.

Ea: the apparent activation energy

The values obtained from the slope of the linear plots are presented in Table 8.

The linear regression coefficient is near to 1, show that the Aluminum alloy corrosion in NaCl 3.5% solution can be explained by the kinetic model. from Table 8, the Ea of inhibitor PS is higher than that of the absence. E_a values in the presence of pumpkin seeds may be read as physical adsorption. A wide energy barrier for the corrosion process in inhibitor presence is related to physical adsorption or low chemical bonding between the molecules of inhibitor and the Aluminum alloy surface [37,38]. The kinetic parameters (ΔS_a entropy of adsorption),(ΔH_a enthalpy of adsorption) obtained from equation 13.

$$Icorr = \frac{RT}{Nh} \exp\left(\frac{\Delta Sa}{R}\right) \exp\left(-\frac{\Delta Ha}{RT}\right) \qquad (13)$$

i_{corr}: the corrosion current density

h: the Plank's constant

N: Avogadro's number

ΔH_a: the enthalpy of activation

ΔSa: the entropy of activation.

Fig.9. present the variation of Ln (i_{corr}/T) as a function of 1/T. The activation parameters (E_a, ΔH_a, and ΔS_a) obtained from the Arrhenius slopes without and with inhibitor pumpkin seeds (Fig.9) are summarized in Table 8.
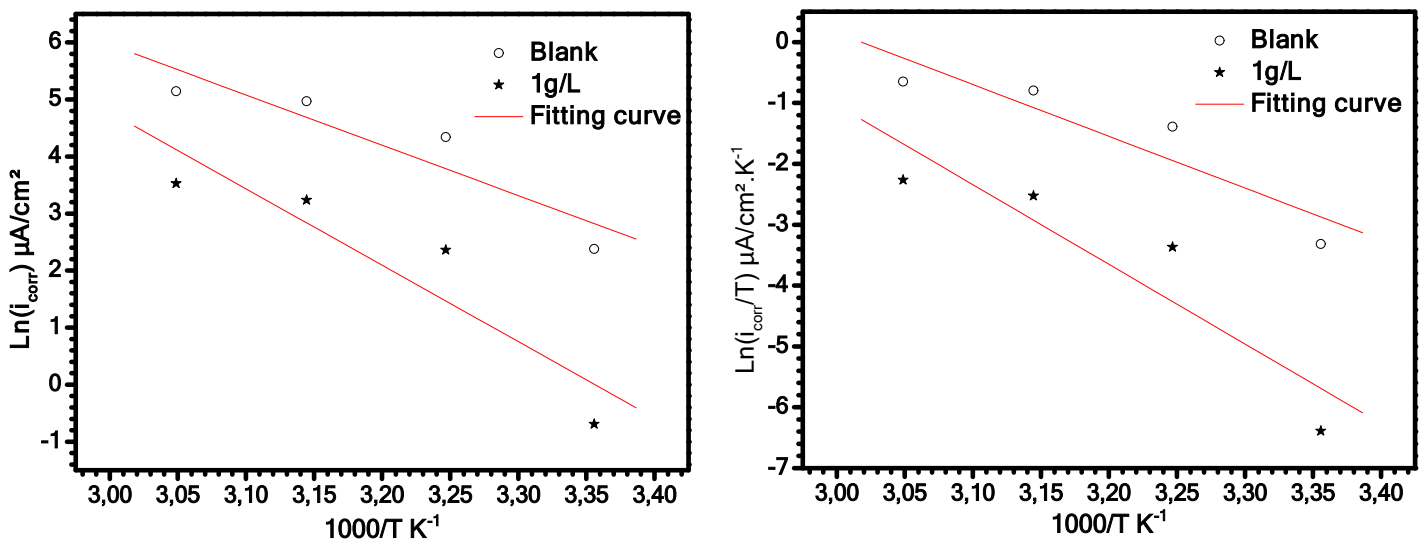
Fig.9. Arrhenius plots of AA7075-T6in NaCl 3,5 % without and with 1g/L of PS.

Table 8. The Values of Ea, ΔHa, and ΔSa for AA7075-T6 in NaCl 3.5% in the absence and presence of PS.

Medium		E_a (Kj/mol)	ΔH_a (Kj/mol)	ΔS_a (Kj/mol)
NaCl 3.5%	BlanK	73.3	70.6	16
	1g/L (PS)	111.4	108.7	120.3

Ea values with a concentration of 1g/L of Pumpkin seeds are higher than the solution without inhibitor. This result of activation energy indicates that the studied inhibitor is adsorbed on aluminum alloy's surface with electrostatic bonds [39,40].The ΔH_a values for Aluminum alloy in NaCl 3.5% in the presence of inhibitor pumpkin seeds (108.7 kJ mol−1) is higher than the absence of inhibitor (70.6kJ mol−1) indicate the dissolution of the Aluminum alloy 7075 is slow [41].Table 8 indicates that the value of ΔS_a increases in the solution inhibited, which signifies that an increase in disorder occurs during the corrosion process to the activated complex [42,43].

3.2.5. Effect of immersion time:

In order to investigate the PS adsorption kinetic and calculate the time needed for PS to reach its maximum efficiency. Fig.10 (a,b) shows the EIS diagrams carried out in the presence and absence of 1g/L of pumpkin seeds in 3.5% NaCl at different immersion times at 298 K in uninhibited and inhibited media.
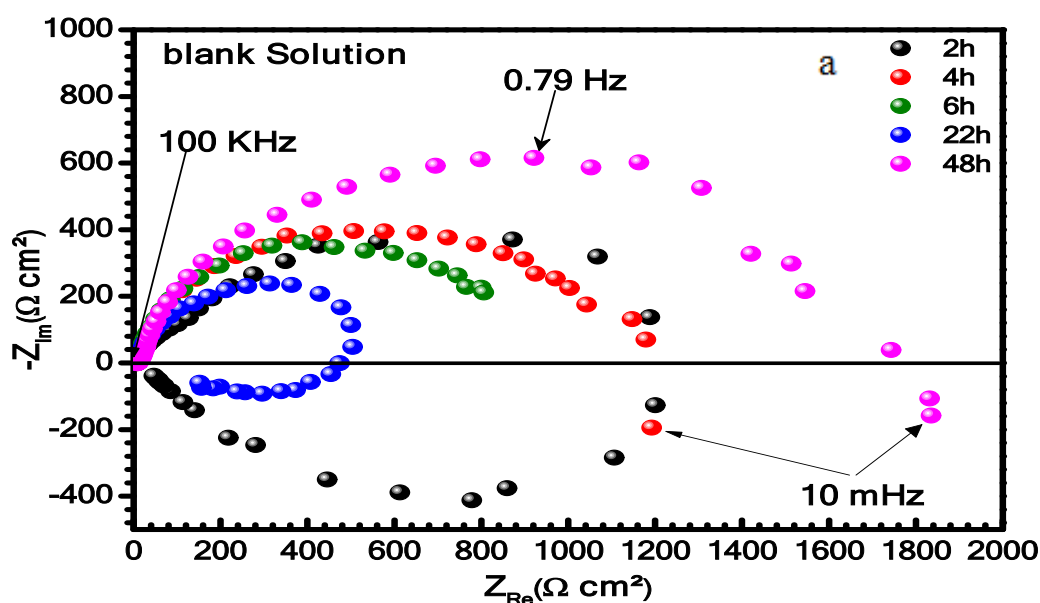
Fig.10. Nyquist diagrams of immersion times of corrosion the AA7075-T6 in NaCl 3.5% at 298 K (a) without inhibitor, (b) with 1g/L of PS.

Fig.11. Nyquist plots of AA7075-T6 immersed in 1g/L of PS in 3.5% NaCl after 2 hours.

The size of the capacitive arc in inhibitor PS is wide than that in the blank solution together with time. The more important data obtained by the equivalent circuit are shown in Table 9.

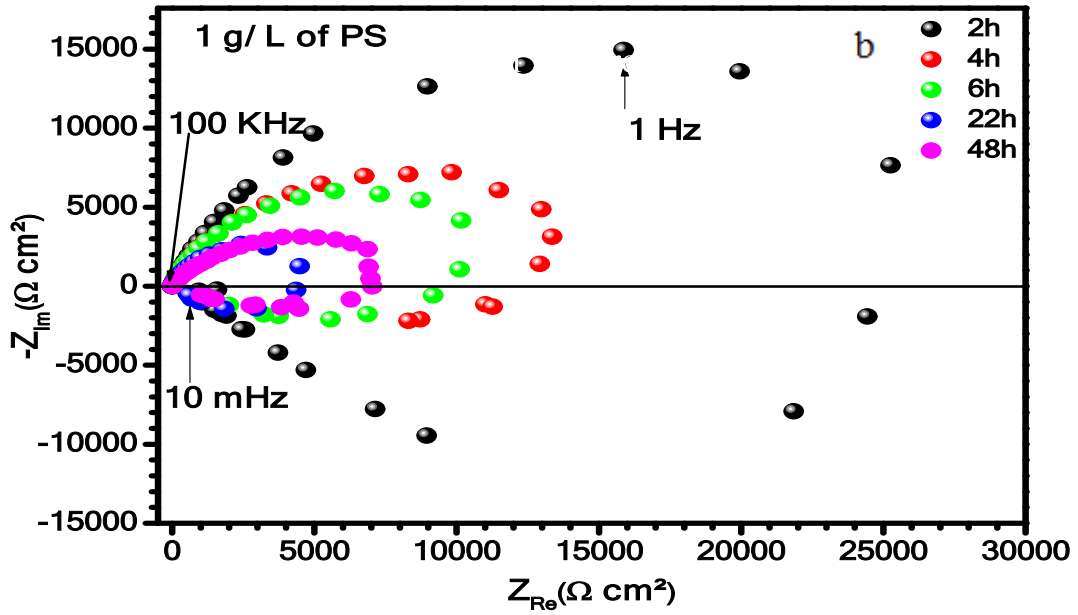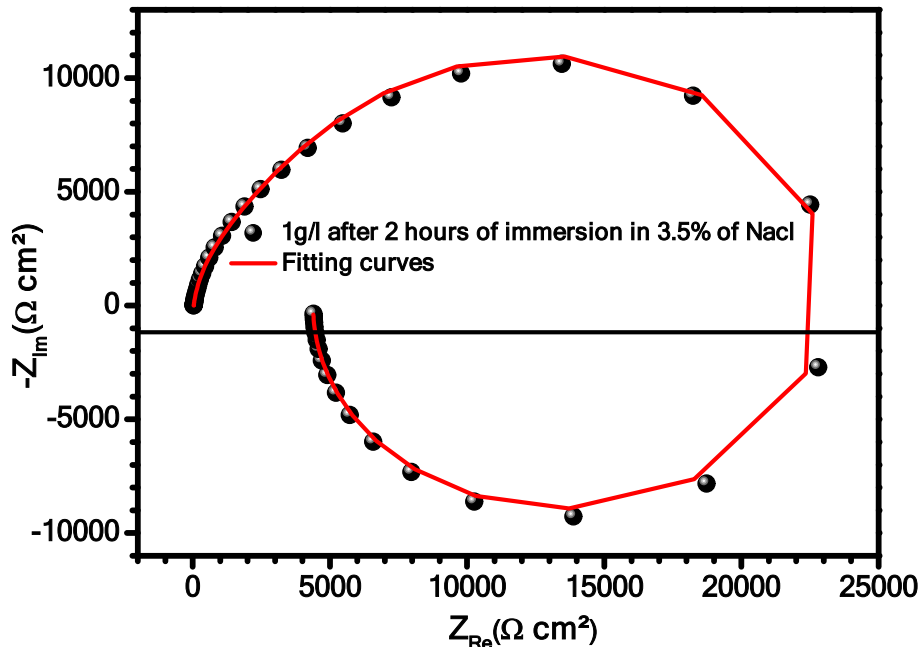**Table 9.** Parameters electrochemical of AA7075-T6 in NaCl 3.5% at 298 K without and with 1g/L of PS at different immersion times

Medium	Temps (h)	R_S	C_f	nF	R_f	Cct	n_{ct}	R_{ct}	R_L	L	R_P	EI%
	2	12.53	172	1	107.3	82.33	0.90	1111	16	211	1230	-
	4	10	105	0.9	815	150	0.85	400	-	-	1215	-
	6	9.5	212	0.45	335	141	0.89	505	-	-	840	-
	22	9	1071	0.95	48	94	0.87	510	284.1	152	558	-
	48	3	111	0.91	741	96	0.88	990	-	-	1731	-
	2	39	12.34	0.9	3691	10.88	0.95	21715	698	6622	25445	95
	4	14	103	0.88	2500	19	0.8	11281	2108	304	13781	91
_	6	20	108	0.81	1205	34	0.82	9850	5500	606	11055	92
	22	14.5	232	0.79	998	85	0.72	3850	2038	295	4850	88.5
	48	13.5	145	0.77	1650	100	0.72	5450	4025	630	7100	76

R_s, R_{ct}, R_f, R_L and R_p ,are expressed in $\Omega.cm^2$

C_f ,C_{ct} are given in $\mu F\ cm^{-2}$

QfandQct are expressed $\mu F\ cm^{-2}.S$

L is expressed in H.

From EIS data, it is evident that the Rp value decreased during the initial 2 h ($25.4 K\Omega.cm^2$) then increases until 48 h the value of Rp ($7.1 K\Omega.cm^2$). The results reveal that IE % decreases slightly with increasing immersion time for the initial 2 h (from 95 to 88.5%). This is coherent with synergistic inhibitor action due to adsorption on aluminum alloy's surface **[44].**

The appearance and disappearance of the inductive loop at low frequencies during the immersion time can be attributed to the adsorption/desorption phenomena at the level of the passive layer's defects or inhibitor layer formed on the metal surface **[45].**

3.3. Surface analysis

3.3.1. Scanning electron microscopy (SEM):

In the absence and presence of the inhibitor PS, the 7075 aluminum alloy's surface morphologies in 3.5% NaCl solution were analyzed by the Scanning electron microscopy (SEM) images, and the surface compositions were identified from their EDX spectra.Fig.12 (a,b) shows the SEM images and the corresponding EDX of the corroded and inhibited surface of the AA7075-T6 following 2 hours of immersion in 3.5% NaCl solution. Fig 13 present the SEM images and the corresponding EDX of the inhibited surface of the AA7075-T6 after 20 hours. The results EDX are summarized in table 10.
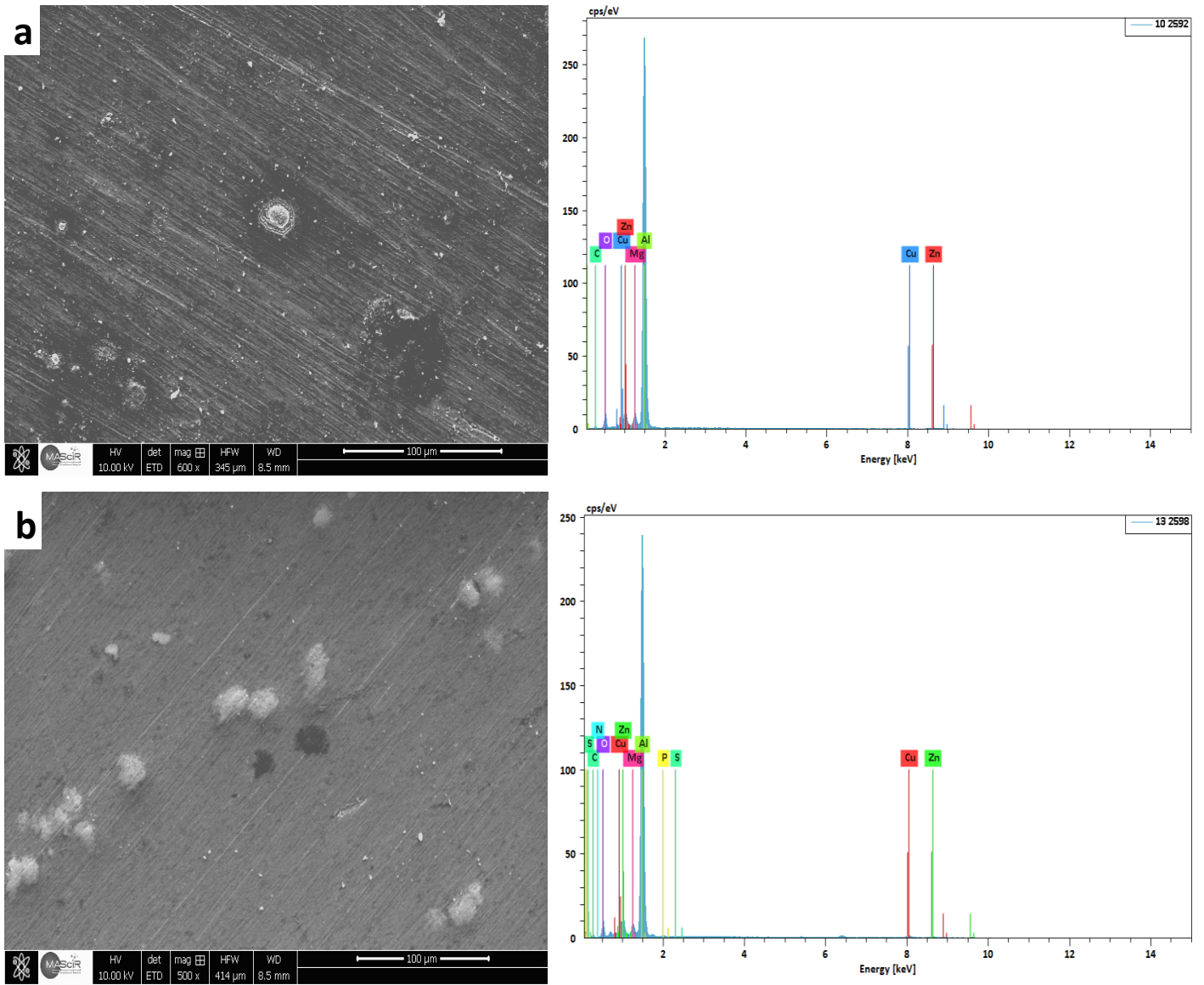
Fig .12. Surface morphology and Quantitative EDAX analysis of AA7075-T6 after immersion for 2h in 3.5% NaCl **(a)** without inhibitor **(b)** with PS 1 g/L.
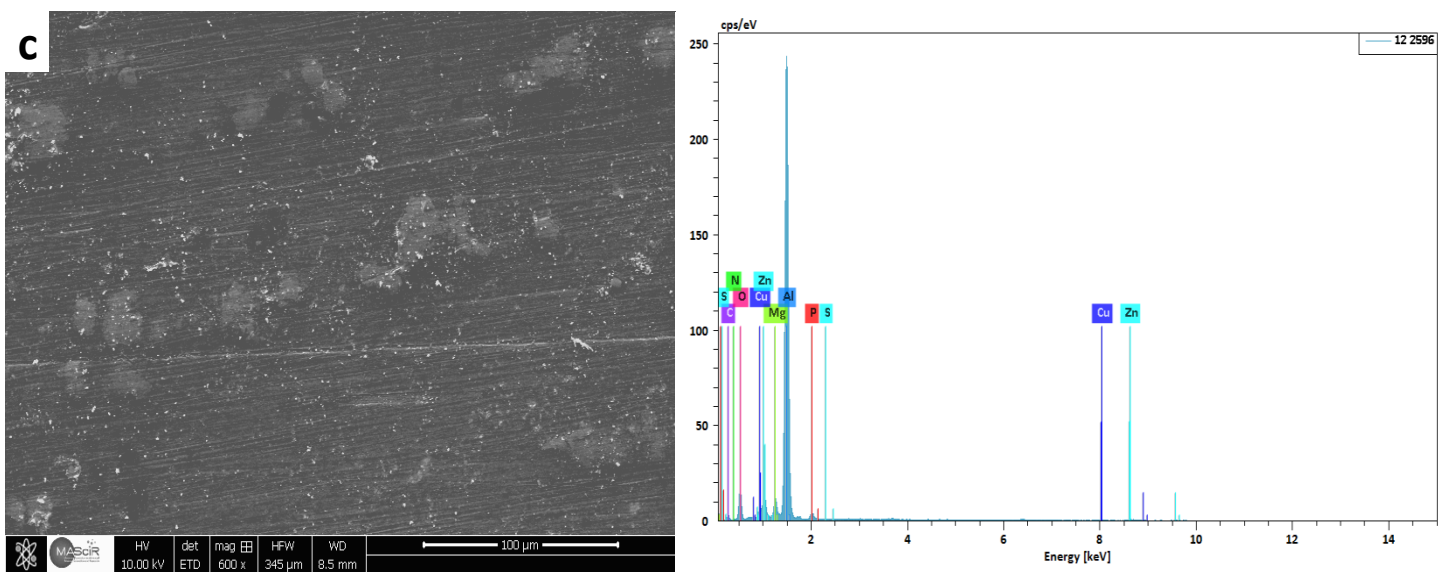

Fig .13. Surface morphology and Quantitative EDAX analysis of AA7075-T6 after immersion for 20h in 3.5% NaCl with PS 1g/L.

The SEM image of 7075-T6 without inhibitor Fif.12 (a) present intense degradation around the intermetallic particles. In the presence of inhibitor PS (Fig.12.b and 13), the surface without any grave corrosion attack. We can observe the appearance of a protective layer thicker and intense.

Table 10. The EDX analysis of the corrosion products formed on AA7075-T6.

Element	Blank	PS (2h)	PS (20h)
Carbon	9.40	12.20	15.55
Nitrogen	-	**1.53**	**1.29**
Oxygen	16.70	11.26	20.63
Magnesium	2.19	2.18	2.47
Aluminum	53.01	67.93	56.55
Phosphorus	-	**0.23**	**1.10**
Sulfur	-	**0.02**	**0.03**
Copper	0.49	2.10	0.71
Zinc	2.52	1.28	1.23

The EDX analysis of the corrosion products formed on AA7075-T6 is shown in Table 10. Table 10 shows the phase $MgZn_2$ was the major intermetallic phase detectable in the microstructure. Nitrogen N and Sulfur S peaks' appearance indicate that the minority compounds of PS presented in table 3 are also adsorbed on the alloy surface [46,47].the presence of phosphorus P is attributed to the presence of diverse bioactive compounds including vitamins (E,D,K) [48,49], vitamin B group (vitamin B1($C_{63}H_{88}CoN_{14}O_{14}P$))[50], minerals (P,Ca,Mg,Fe,Cu,Mn,Se 0,08 to 0,4 mg/g) [51,52].As a consequence, these results justify those obtained from electrochemical measurements.

3.3.2 Atomic force microscope (AFM):

Atomic Force Microscopy (AFM) is a powerful technique that examines surface morphology at the micron and nanometer scales, the formation of the adsorbed "barrier" layer, and the effects of inhibitors at the interface. metal /solution[53-57]. Micrographs of the AA7075-T6 surface immersed in 3.5% NaCl in the absence and presence of PS 1g/L are shown in three dimensions: Fig.14 (a,b).
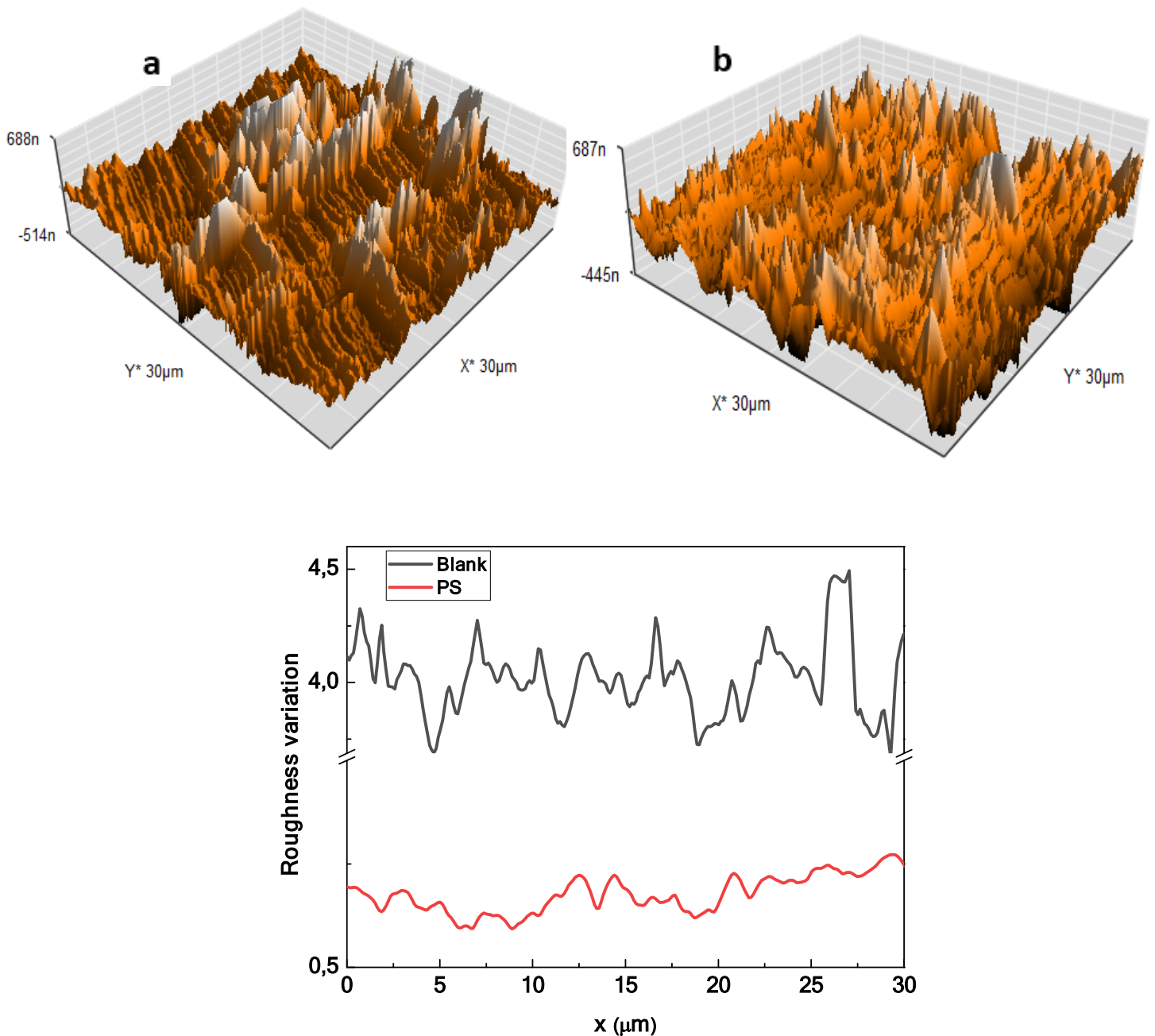
Fig.14. AFM images and Roughness variation after 24 hours of immersion of AA7075-T6 in 3.5% NaCl: **(a)** in the absence and **(b)** in the presence of PS1g / L.

The major difference observed between the two images is the protective layer on the inhibited surface (Fig.14.b), attributed to the adsorption of inhibitor molecules to the surface of 7075-T6 aluminum. While, the surface of AA7075-T6 in the uninhibited corrosive solution (Fig.14.a) is severely damaged. The Arithmetic Average Roughness denoted **(Ra)** indicates the average roughness of the surface for the length of the measurement made, that is to say, the average difference between the peaks and the valleys. The values of the average surface roughness Ra of the two samples are summarized in Table 11.

Table 11. The average surface roughness values derived from the AFM analysis of the surface of AA7075-T6 in 3.5% NaCl solution in the absence and presence of PS 1 g /L.

Sample	AA7075 NaCl 3.5%	AA7075 NaCl 3.5%+PS1g/L
Ra (nm)	338	103

The result obtained on 30 x 30 μm² images shows that the surface roughness (**Ra**) is 338 nm for the uninhibited AA 7075-T6 surface. The addition of PS 1g/L reduces the average roughness value (**Ra**) at 103 nm due to the formation of a protective layer on the aluminum surface.

3.3.2 X-ray diffraction analysis:

The X-ray diffraction measurements of AA7075-T6 were performed to identify the corrosion products formed on the specimen surface. The XRD patterns of AA7075-T6 with and without inhibitor in 3.5% NaCl solution after 20 h are represented in Fig. 15.
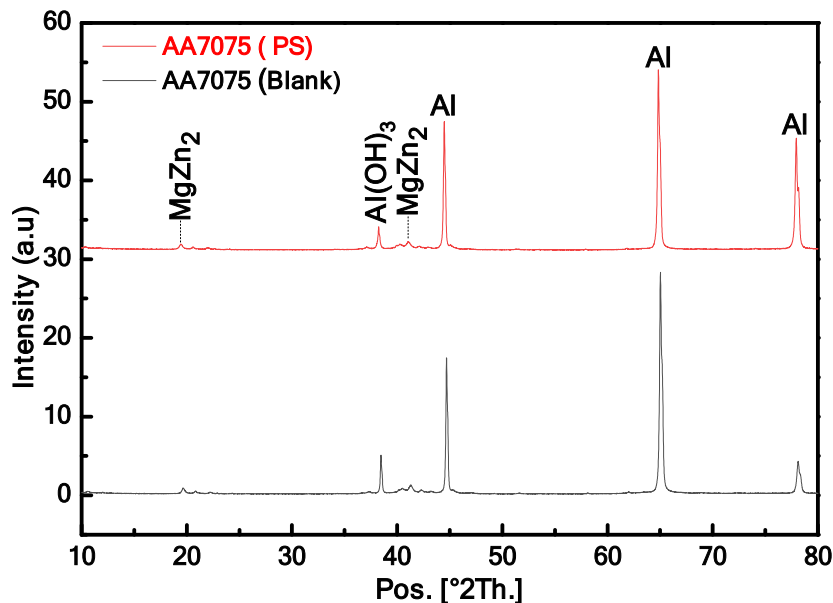
Fig. 15. XRD patterns of AA7075-T6 in NaCl 3.5% with and without PS

Three major peaks were identified as Al with higher intensity. Two peaks corresponded to the $MgZn_2$ phase, and $Al(OH)_3$ with lower intensity values. A very small intensity peak corresponding to the $MgZn_2$ precipitate is observed without any other intermetallic compounds. The intensity of $Al(OH)_3$ peaks decreases in the presence of PS, suggesting that protection is formed with inhibitor **[58-60].**

There may be some other compositions present in PS which XRD cannot detect. The theoretical calculations would help us to explain it.

3.4. Computational study

Optimized, HOMO and LUMO

palmitic acid and linoleic acid derived through Gaussian 09 software are presented in Figure 16 and numerous DFT parameters are presented in Table 12.

Fig.16. Optimized, HOMO and LUMO molecular orbital pictures of Z,Z)- 9,12-Octadecadienoic acid, palmitic acid and linoleic acid derived through Gaussian 09 software.

Table 12.DFT parameters derived for (Z,Z)- 9,12-Octad-ecadienoic, palmitic acid and linoleic acid calculated using Gaussian 09 software.

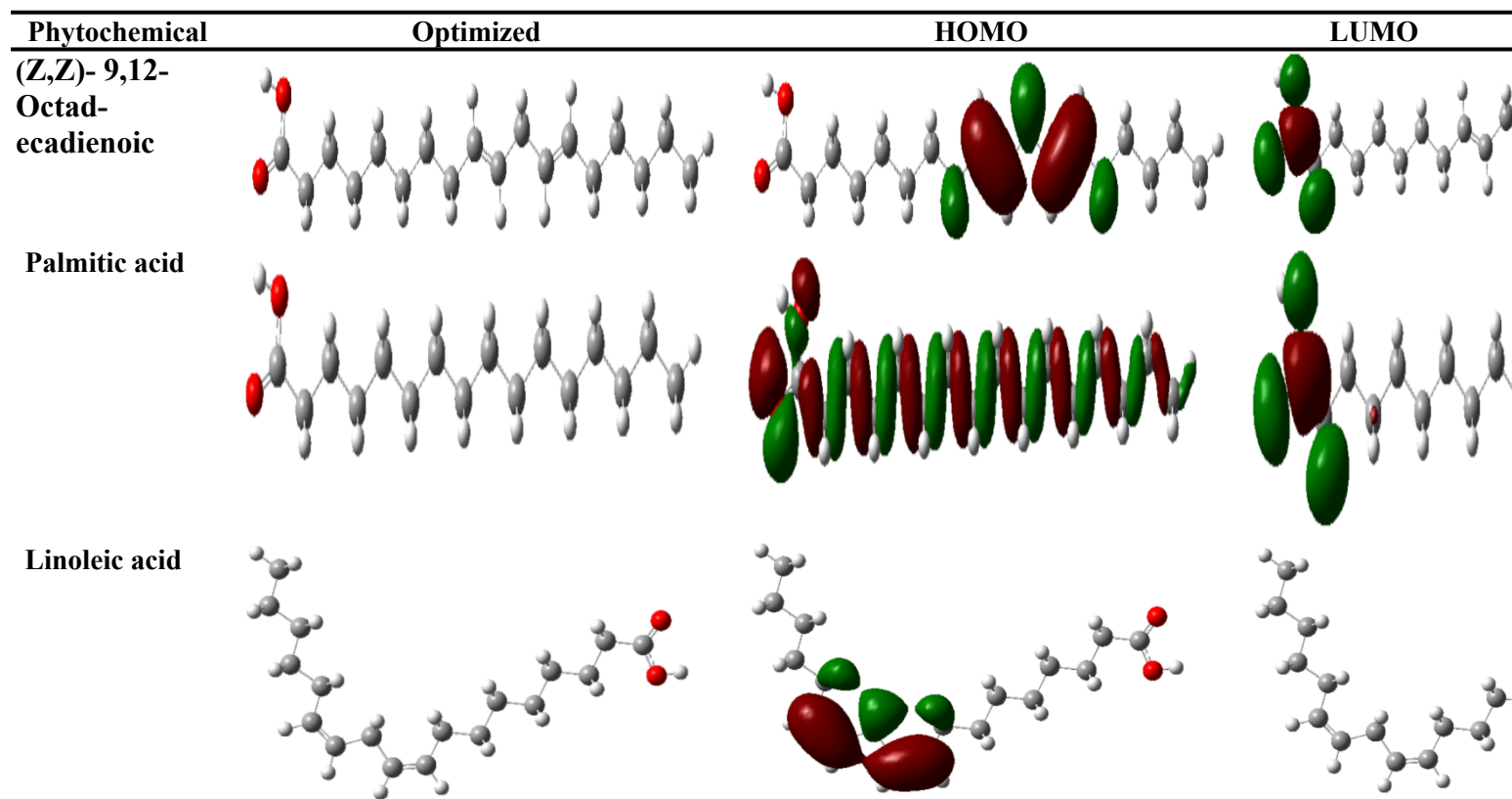| Phytochemical	E_{HOMO} (eV)	E_{LUMO} (eV)	ΔE (eV)	IP	EA	η	χ	σ	ΔN	μ (Debye)
Palmitic acid	-7.293	-0.178	7.115	7.293	0.178	3.557	3.735	0.281	0.152	1.717
Linoleic acid	-6.226	0.055	6.281	6.226	-0.055	3.140	3.085	0.318	0.276	1.298
(Z,Z)- 9,12-Octad-ecadienoic	-5.940	0.066	6.006	5.940	-0.066	3.003	2.937	0.333	0.313	1.702

It can be seen that FMOs (HOMO and LUMO) are localized over some specific parts of the molecules. These parts are responsible for charge sharing with the metallic surface. It is assume that localized regions in HOMO are responsible for electron donation and localized regions in LUMO are responsible for electron acceptance [30, 61-63]. In (Z,Z)- 9,12-Octad-ecadienoic and linoleic acid, HOMO is localized over the double bond(s) indicating that these molecules transfer their π-electrons into the empty orbitals of surface aluminum atoms. On the other hand, HOMO in palmitic acid is localized over the hydrocarbon chain. Careful observation of the Figure 16 shows that LUMO is localized over carboxylic functional group

(–COOH) in all investigated phytochemicals indicating that –COOH moiety is mainly involves in charge acceptance because of its electron withdrawing ability.

Obviously, E_{HOMO} represents ability of a molecule to donate its electrons to an appropriate acceptor molecule. Therefore, a high value of E_{HOMO} is associated with higher inhibition efficiency. Investigation of the results presented in Table 12, shows that values of E_{HOMO} are increasing (in positive) on moving top to bottom i.e. palmitic acid has lowest value of E_{HOMO} and (Z,Z)- 9,12-Octad-ecadienoic has its highest value. This observation suggests that (Z,Z)- 9,12-Octad-ecadienoic is the best phytochemical and palmitic acid is the least effective anticorrosive phytochemical. The linoleic acid acquires the intermediate position. Conversely, E_{LUMO} denotes the electron accepting property of a molecule and its lower value is associated with high chemical reactivity as well as high corrosion inhibition potential. Outcomes presented in Table 12 show that values of E_{LUMO} for (Z,Z)- 9,12-Octad-ecadienoic, palmitic acid and linoleic acid don't exhibit any regular trends. Energy band gap, ΔE (E_{LUMO}-E_{HOMO}) is another reactivity parameter in the term of which corrosion inhibition potential of an organic compound can be described. Obviously, a lesser value of ΔE is consistent with high chemical reactivity and corrosion inhibition potential and vice versa. Observation of the ΔE values presented in Table 12 shows that (Z,Z)- 9,12-Octad-ecadienoic acquires the lowest value of ΔE whereas palmitic acquires its highest value. This observation further suggests that (Z,Z)- 9,12-Octad- ecadienoic is the best and palmitic acid is the least effective phytochemicals. Values of ionization potential (IP) and electron affinity (EA) are consistent with the values of E_{HOMO} and E_{LUMO}, respectively.

Generally, a lower value of hardness (η) and electronegativity (χ) are associated with high chemical reactivity as well as high inhibition potential [30-32]. Results shows that (Z,Z)- 9,12-Octad-ecadienoic has lowest values of hardness and electronegativity therefore it would be most effective anticorrosive species among the investigated phytochemicals. On the other hand, converse is true for palmitic acid, which is the least effective species. Lastly, values of global softness (σ) were also derived for (Z,Z)- 9,12-Octad- ecadienoic, palmitic acid and linoleic acid. Generally, a chemical species having smaller value of global softness is associated with high chemical reactivity and corrosion inhibition potential and vice versa. Results presented in Table 12 shows that (Z,Z)- 9,12-Octad- ecadienoic is the most effective anticorrosive species and palmitic acid is the least effective chemical species. Magnitude of dipole moment (μ) don't show any regular trends. On the basic of above discussions, effectiveness of the phytochemicals investigated through DFT studies followed the sequence: (Z,Z)- 9,12-Octad- ecadienoic > linoleic acid > palmitic acid.

3.5. Mechanism of corrosion/Inhibition AA7075-T6:

The presence of multiple heterogeneities formed during structural hardening of 7000 series aluminum alloys causes a considerable decrease in corrosion resistance properties. These heterogeneities are the source of localized corrosion phenomena [64]. The Al_7Cu_2Fe phase has a corrosion potential superior to that of the matrix of the 7075 alloy. This phase seems to adopt a generally passive character attributed to forming an Al_2O_3 or $Al(OH)_3$ alumina layer by certain authors [65].In alloy 7075, the matrix adjacent to the Al_7Cu_2Fe particle will preferably be dissolved compared to the Al_2Cu phase.

According to Birbilis, the alloy matrix's corrosion potential is stable around -0.75 V/ECS [66] at this potential, the Al_7Cu_2Fe phase is cathodically polarized. The exchange current associated with the reduction of oxygen is high. Compared with the Al_2Cu phase, the rate of oxygen reduction in the Al_7Cu_2Fe phase is three times higher, indicating greater cathodic activity. This phenomenon is attributed to the presence of copper and iron in the phase. The local formation of OH^- ions (local increase in pH), due to the significant reduction in oxygen on the Al_7Cu_2Fe phase, seems to help increase the rate of dissolution of the surrounding matrix (cathodic corrosion) [67].Overall, the electrochemical behavior of the Al_7Cu_2Fe phase is similar to that of the Al_2Cu phase, with the only exception that the presence of iron catalyzes the oxygen reduction[68].In contrary to the majority of cathodic-type intermetallic phases (Al_2Cu and Al_7Cu_2Fe), $MgZn_2$ particles seem to have an active behavior in chloride medium with a potential between -1 and -1.05 V / ECS [69,70].It should be noted that this type of particle progressively oxidizes with increasing potential.

The $MgZn_2$ phase has an inferior corrosion potential than that of the matrix of the 7000 alloy. Furthermore, the corrosion current of the $MgZn_2$ phase is superior to that of the matrix. The corrosion kinetics of 7075 aluminum alloy is governed on one part by the anodic process, the dissolution of the matrix, and on the other part by the reduction of dissolved oxygen. Corrosion takes place at the null current of the sum of these two processes. The electrochemical and theoretical results obtained showed that PS capable of significantly and notably reducing the rate of corrosion limiting the two reactions: the cathodic reaction taking place on the intermetallic phases rich in Cu and Zn, seats of the reduction of dissolved oxygen, and the anodic reaction, seat of the dissolution of the surrounding matrix.
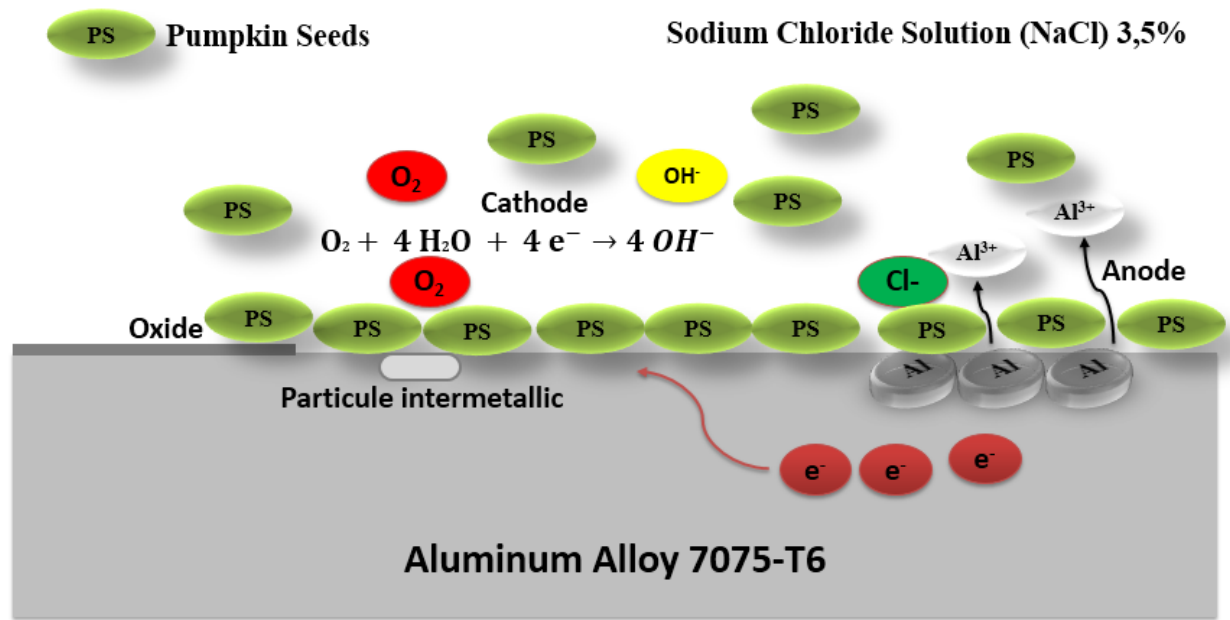
Fig.17. Schematic representation of the corrosion/protection mechanisms for AA7075-T6 in the presence of PS.

4. CONCLUSIONS

The corrosion inhibition efficiency of AA7075-T6 in NaCl 3,5% by Pumpkin seeds has been investigated utilizing electrochemical measurement, surface analysis, and theoretical studies. The following conclusions were drawn from the study:

- PS serves as a good inhibitor for aluminum alloy 7075-T6 corrosion in 3.5% NaCl solution.
- Inhibition efficiency of PS increases on increasing its concentration and maximum values of inhibition efficiency of 95% was obtained at 1g/L.
- Tafel polarization study suggests that PS acts as a cathodic type inhibitor.
- Adsorption of pumpkin seeds on the AA7075-T6 surface was consistent with the Langmuir adsorption isotherm.
- Thermodynamic parameters show that PS effectively and spontaneously adsorbs on the aluminum surface.
- Decrease in the protection efficiency was observed with rise in the immersion time.
- Results derived from SEM/EDAX, AFM, and XRD analyses were consistent with the results of PDP and EIS studies.
- Experimental and computational results were in good agreement.

References

[1] C.Vargel, Corrosion de l'aluminium. s.l. : Dunod, 1999.

[2]N.Kamp,I.Sinclair, and M.J.Starink, Toughness-Strength Relations in the Overaged 7449Al-Based Alloy, Metallurgical And Materials TransactionsA33 (2002) 1125-1136.

[3]N.Birbilis,M.K.Cavanaugh,andR.G.Buchheit, Electrochemical behavior and localized corrosion associated with Al7Cu2Fe particles in aluminum alloy 7075-T651, Corrosion Science 48 (2006) 4202-4215.

[4] Z.Li, B.Xiong,Y.Zhang, B.Zhu, Wang.F, and H.Liu, Investigation on strength, toughness and microstructure of an Al–Zn–Mg–Cu alloy pre-stretched thick plates in various ageing tempers, Journal of materials processing technology 209 (2009) 2021-2027.

[5] F.Andreatta,H.Terryn, and J.H.W.De Wit, Effect of solution heat treatment on galvanic coupling between intermetallics and matrix in AA7075-T6, Corrosion Science 45 (2003) 1733-1746 .

[6] L. Bazzi, S. Kertit and M. Hamdani. Rev Metall92(1995)690.

[7] B.A. Shaw, G.D. Davis, T.L. Fritz and K.A. Olver. J. Electrochem. Soc 137(1990)350.

[8]A.Ostovari, S.M.Hoseinieh, M.Peikari, S.R.Shadizadeh, and S.J.Hashemi, Corrosion Science51 (2009) 1935–1949.

[9] O. K.Abiola, and Y.Tobun Chinese Chemical Letters 21 (2010) 1449–1452.

[10] KM.Phillips, DM.Ruggio, and M.J.Ashraf-Khorassani Agric Food Chem 53 (2005) 9436-9445.

[11]W.L.Applequist, B.Avula, B.T.Schaneberg, Y.H.Wang, and I.A.Khan. Comparative fatty acid content of seeds of four Cucurbita species grown in a common (shared) garden. J Food Composition and Analysis (2006) 19606–19611.

[12]R.H.Glew,R.S.Glew, L.T.Chuang, Y.S.Huang, M.Millson, D.Constans,and D.J .Vanderjagt Plant Foods Hum Nutr 61 (2006) 51-6.

[13] A.Bouckamp, Users Manual Equivalent Circuit (1993) Ver. 4.51.

[14] I. Obot, D. Macdonald, Z. Gasem, Density functional theory (DFT) as a powerful tool for designing new organic corrosion inhibitors. Part 1: an overview, Corrosion Science, 99 (2015) 1-30.

[15] G. Gece, S. Bilgiç, Quantum chemical study of some cyclic nitrogen compounds as corrosion inhibitors of steel in NaCl media, Corrosion Science, 51 (2009) 1876-1878.

[16] D.K. Verma, Density functional theory (DFT) as a powerful tool for designing corrosion inhibitors in aqueous phase, Advanced Engineering Testing (2018) 87.

[17]T.Chipiti, M.A.Ibrahim, N.A.Koorbanally, and S.Islam, Acta Polytech.Scand, Chem. Technol. Ser (2015) 72.

[18] M.A.Elhassan, H. S. Ahmed Hoyam, H.A.Samia, M. E. KhogaliSalwa, GC.MS Analysis of Pumpkin Seeds (Cucurbita maxima, Cucurbitaceae). Archives of Business Research8 (2018) 1-9

[19] R.C.B.Cruz,C.D.Meurer, EJ.Silva, et al,Toxicity evaluation of Cucurbita maxima seed extract in mice. Pharm Biol 44 (2006) 301-3.

[20] A.Queiroz-Neto, M.I.Mataqueiro, A.E.Santana, A.C.Alessi, Toxicologic evaluation of acute and subacute oral administration of Cucurbita maxima seed extracts to rats and swine. J Ethnopharmacol, 43 (1994)45-51.

[21] J.Raynaud, Prescription et Conseil En Phytothérapie, TEC ET DOC, Paris (2006) 101-103.

[22] S.Ambrish,L.Yuanhua , L.Wanying , Y.Shijie, P.Jie , and R.Chengqiang , Deng Kuanhai Plant derived cationic dye as an effective corrosion inhibitor for 7075 aluminum alloy in 3.5% NaCl solution ,Int. J. Electrochem. Sci (2014) 5560 – 5573.

[23] H.Gerengi.Anticorrosive Properties of Date Palm (Phoenix dactylifera L.) FruitJuice on 7075 Type Aluminum Alloy in 3.5% NaCl Solution.Ind. Eng. Chem. Res 51(2012) p 12835−12843.

[24]M. A. Amin, S. S. Abd El-Rehim, E. F. El-Sherbini, and R. S. Bayyomi, Electrochim. Acta 52(2007)3588.

[25]M. Lebrini, F. Robert, A. Lecante, and C. Roos, Corros. Sci53(2011)687.

[26]W.C Chen, T.C Wen, and A. Gopalan, Role of anions to influence inductive behaviour for poly(2-amino diphenylamine-co-aniline) – an electrochemical impedance spectroscopic analysis, Synthetic Metals 130 (2002) 61-71.

[27]A. Dehghani, G. Bahlakeh, B. Ramezanzadeh, A detailed electrochemical/ theoretical exploration of the aqueous Chinese gooseberry fruit shell extract as a green and cheap corrosion inhibitor for mild steel in acidic solution, J. Mol. Liq. 282 (2019) 366–384

[28]A. Popova, E. Sokolova, S. Raicheva,and M. Christov, Corros. Sci45 (2003) 33–58.

[29]M. Goyal, S. Kumar, I. Bahadur, C. Verma, E. E. Ebenso, Organic corrosion inhibitors for industrial cleaning of ferrous and non-ferrous metals in acidic solutions: A review, Journal of Molecular Liquids. 256 (2018) 565–573.

[30]O.Kassou, and al. "Comparative study of low carbon steel corrosion inhibition in 200 ppm NaCl by amino acid compounds." J. Mater. Environ. Sci (2015)1147-1155.

[31] Oguzie and al, 2007; Sharma and al,2008.

[32]G. Moretti, F. Guidi, G. Grion, Corros. Sci 46(2004) 387–403.

[33]R. Hasanov, S. Bilge, S. Bilgic, G. Gece,and Z. Kilic, *Corros. Sci*52 (2010) 984–990.

[34]V.S. Sastri, Green Corrosion Inhibitors: Theory and Practice, John Wiley &Sons, (2012).

[35]U.F. Ekanem, S.A. Umoren, I.I. Udousoro, A.P. Udoh, and J. Matter.Sci 45(2010) 5558-5566.

[36]I. Ahamad, R. Prasad, and M.A. Quraishi, Corros Sci 52(2010)3033-3041.

[37]A. Popova, E. Sokolova, S. Raicheva, and M. Christov, AC and DC study of the temperature effect on mild steel corrosion in acid media in the presence of benzimidazole derivatives,Corros. Sci, 45(2003) 33–58.

[38] M. Elayyachy, M. Elkodadi, A. Aouniti, A. Ramdani, B. Hammouti, F. Malek, and A.Elidrissi, New bipyrazole derivatives as corrosion inhibitors for steel in hydrochloric acid solutions, Mater. Chem. Phys.93(2005)281–285.

[39]A.Bousskri, R. Salghi, Anejjar, M. Messali, S. Jodeh, O. Benali, M. Larouj, I. Warad, O. Hamedc, and B. Hammouti, Portugaliae Electrochim. Acta 34(2016) 1–21.

[40] A. Zarrouk, B. Hammouti, H. Zarrok, R. Salghi, A. Dafali, Lh. Bazzi, and L. Bammou, S.S. Al-Deyab, Der Pharma Chem4 (2012)337-346.

[41]N.M.Guan , L.Xueming ,and L.Fei , Mater. Chem. Phys86 (2004)59.

[42]A.K. Singh, and M.A. Quraishi, Investigation of the effect of disulfiram on corrosion of mild steel in hydrochloric acid solution, Corros. Sci,53(2011)1288–1297.

[43]M. Yadav, S. Kumar, N. Tiwari, I. Bahadur, E. E. Ebenso, Experimental and quantum chemical studies of synthesized triazine derivatives as an efficient corrosion inhibitor for N80 steel in acidic medium, J Mol Liq. 212 (2015) 151–67

[44]M.A. Ameer, and A.M. Fekry.Inhibition effect of newly synthesized heterocyclic organic molecules on corrosion of steel in alkaline medium containing chloride.International journal of hydrogen energy35(2010)11387 -11396.

[45]A.Y. Musa, A.B.Mohamad, A.H Kadhum, and Y.BashirA.Tabal Inhibition of Aluminum Alloy Corrosion in 0.5 M NitricAcid Solution by 4-4-Dimethyloxazolidine-2-thione. Journal of Materials Engineering and Performance20(2011)394–398

[46]A. S. Fouda, Mohamed A. Ismail, A. A. Al-Khamri, A. S. Abousalem., Experimental, quantum chemical and molecular simulation studies on the action of arylthiophene derivatives as acid corrosion inhibitors, Journal of Molecular Liquids. 290 (2019) 111178

[47]Z.Y.Cui, X.G. Li, K. Xiao, C.F. Dong, L.W. Wang, D.W. Zhang, and Z.Y. Liu Exfoliation Corrosion Behavior of 2B06 Aluminum Alloyin a Tropical Marine Atmosphere.Journal of Materials Engineering and Performance 24(2015)296–306

[48] M.Nishimura, T.Ohkawara, H.Sato, H.Takeda, J.Nishihira, Pumpkin Seed Oil Extracted From Cucurbita maxima Improves Urinary Disorder in Human Overactive Bladder Journal of Traditional and Complementary Medicine (2014) Vo1. 4, No. 1, pp. 72‐74

[49]G.Fruhwirth, A. Hermetter Seeds and oil of the Styrian oil pumpkin: Components and biological activities European Journal of Lipid Science and Technology ,2007.

[50]E.H Mansour,E.Dworschak, A.Lugasi, E.Barna and A.Gergely, Nutritive Value of Pumpkin (Cucurbita pepoKakai 35) Seed Products, J Sci Food Agric 61 (1993) 73-78

[51] P. Goetz, R. Le Jeune, Huile de graine de courge, Cucurbita pepo convar.citrullina var. styriaca , Springer-Verlag France 8 (2010) 136–140.

[52] G.O.Fruhwirth, A.Hermetter, Production technology and characteristics of Styrian pumpkin seed oil, Eur. J. Lipid Sci. Technol. 110 (2008) 637–644

[53] R.Fuchs-Godec, G.Miomir, Pavlovic."Synergistic effect between non-ionic surfactant and halid ions in the forms of inorganic or organic salts for the corrosion inhibition of stainless-steel X4Cr13 in sulphuric acid". Corros.Sci 58(2012)192-201

[54] R. Solmaz, G. Kardas_, M. Culha, B. Yazıcı, M. Erbil, Investigation of adsorption and inhibitive effect of 2-mercaptothiazoline on corrosion of mild steel in hydrochloric acid media, Electrochim. Acta 53 (2008)5941–5952

[55] R.Solmaz, Investigation of the inhibition effect of 5-((E)-4-phenylbuta-1,3-dienylideneamino)-1,3,4-thiadiazole-2-thiol Schiff base on mild steel corrosion in hydrochloric acid, Corros. Sci. 52 (2010)3321–3330.

[56] S.A. Umoren, Y. Li, F.H. Wang, Electrochemical study of corrosion inhibition and adsorption behaviour for pure iron by polyacrylamide in H2SO4: synergistic effect of iodide ions, Corros. Sci. 52 (2010) 1777–1786.

[57] B. Wang, M. Du, J. Zhang, C.J. Gao, Electrochemical and surface analysis studies on corrosion inhibition of Q235 steel by imidazoline derivative against CO2 corrosion, Corros. Sci. 53 (2011) 353–361.

[58] Y.Wu, Y.Zhang, Y. Jiang, Y.Qian, X.Guo, L.Wang, J.Zhang, Orange peel extracts as biodegradable corrosion inhibitor for magnesium alloy in NaCl solution: Experimental and theoretical studies Journal of the Taiwan Institute of Chemical Engineers 000 (2020) 1_12.

[59] H.Su, L.Wang, Y.Wu, Y.Zhang, J.Zhang Insight into inhibition behavior of novel ionic liquids for magnesium alloy in NaCl solution: Experimental and theoretical investigation,J.Corrosion Science (2019).

[60] H.Su, Y.Wu, Y.Zhang, Y. Jiang, Y.Ding, L.Wang, J.Zhang, Enhancing the long-term anti-corrosion property of Mg alloy by quaternary phosphonium salt: Integrated experimental and theoretical approaches, J.Corrosion Science 2020.

[61] C. Verma, L.O. Olasunkanmi, E.E. Ebenso, M.A. Quraishi, I.B. Obot, Adsorption behavior of glucosamine-based, pyrimidine-fused heterocycles as green corrosion inhibitors for mild steel: experimental and theoretical studies, The Journal of Physical Chemistry C, 120 (2016) 11598-11611.

[62] C. Verma, E. Ebenso, I. Bahadur, I. Obot, M. Quraishi, 5-(Phenylthio)-3H-pyrrole-4-carbonitriles as effective corrosion inhibitors for mild steel in 1 M HCl: experimental and theoretical investigation, Journal of Molecular Liquids, 212 (2015) 209-218.

[63] I. Obot, S. Kaya, C. Kaya, B. Tüzün, Density Functional Theory (DFT) modeling and Monte Carlo simulation assessment of inhibition performance of some carbohydrazide Schiff bases for steel corrosion, Physica E: Low-dimensional Systems and Nanostructures, 80 (2016) 82-90.

[64] Z. Szklarska-Smialowska : Pitting corrosion of aluminum. Corros. Sci., 41(9) (1999) 1743–1767.

[65]R.R Leard, R.G Buchheit, Electrochemical characterization of copper-bearing intermetallic compounds and localized corrosion of Al-Cu-Mg-Mn alloy 2024, Materials Science Forum 396-402 (2002) 1491-1496.

[66] N. Birbilis, M.K Cavanaugh, R.G Buchheit, Electrochemical behaviour and localized corrosion associated with Al7Cu2Fe particles in aluminum alloy 7075-T651, Corrosion Science 48 (2006) 4202-4215.

[67] T.J.R Leclère, R.C Newman, Self-regulation of the cathodic reaction kinetics during corrosion of AlCu alloys, Journal of the Electrochemical Society 149 (2002) B52-B56.

[68] F. Andreatta, H. Terryn, Use of scanning Kelvin probe force microscopy and microcapillary cell to investigate local corrosion behaviour of 7XXX aluminum alloys, European Federation of Corrosion Publications (2007) 126-136.

[69] N. Birbilis, R.G Buchheit, Electrochemical characteristics of intermetallic phases in aluminum alloys, Journal of The Electrochemical Society 152 (2005) B140-B151

[70] N. Birbilis, R.G Buchheit, Investigation and discussion of characteristics for intermetallic phases common to aluminum alloys as a function of solution pH, Journal of The Electrochemical Society 155 (3) (2008) C117-C126

CRediT authorship contribution statement

M.Radi : Investigation, Writing - original draft, Writing - Review & Editing. **R.Melian** : Investigation, Data Curation. **M.Galai**: Data Curation, Writing - original draft, Writing - Review & Editing. **C.Fernandez**: Investigation, Writing – original draft. **Chandrabhan Verma**: Software, Writing - original draft. **M. EbnTouhami**: Conceptualization, Supervision, Visualization. **N. Dkhireche**: Writing – original draft, Writing - review & editing. **M. Makha**: Software, Data Curation.

Highlights

- Pumpkin seeds (PS) acts as effective inhibitors for aluminum corrosion

- The adsorption of PS followed the Langmuir isotherm model.

-adsorption on the surface is analyzed by AFM and SEM/EDAX, techniques

-Theoretical data provide in-depth understanding of the experimental results.

Declaration of interests

☒The authors declare that they have no known competing financialinterestsor personal relationships that could have appeared to influence the work reported in this paper.

☐The authors declare the following financial interests/personal relationships which may be considered as potential competing interests: